

# Structural and dielectric properties of $(1-x)\text{Pb}(\text{Zr}_{0.53}\text{Ti}_{0.47})\text{O}_3-x\text{GdMnO}_3$ ceramics

Y. Bakhaled<sup>1\*</sup>, L. Hamziou<sup>2</sup>, F. Kahouf, A. H. Hamzaoui<sup>3</sup>, A. Midouni<sup>3</sup>, M. Aillerie<sup>4</sup>

<sup>1</sup>Université de Ouargla, Faculté des Sciences Appliquées, Laboratoire de Dynamique Interaction et Réactivités des Systèmes, BP 511, R. Ghardaïa, Ouargla 30000, Algérie

<sup>2</sup>Université de M'Sila, Faculté de Technologie, Département Socle Commun ST, M'Sila 28000, Algérie

<sup>3</sup>Centre Nationale de Recherches en Sciences des Matériaux, Laboratoire de Valorisation des Matériaux Utiles, Technopôle Borj Cedria BP 73, 8027 Soliman, Tunisie

<sup>4</sup>Université de Lorraine & Centrale Supélec, Laboratoire Matériaux Optiques, Photonique et Systèmes, EA 4423, Paris-Saclay 57070 Metz, France

## Abstract

Ceramics compositions  $(1-x)\text{Pb}(\text{Zr}_{0.53}\text{Ti}_{0.47})\text{O}_3-x\text{GdMnO}_3$  ( $x=0, 0.01, 0.02, 0.03, 0.04,$  and  $0.05$ ) were synthesized by solid-state route and sintered at  $1180\text{ }^\circ\text{C}$  for 2 h. Structural, microstructural, and dielectric properties of the system were investigated. X-ray structural analysis of the materials confirmed their formation in a single phase with a tetragonal crystal structure. The PZT ceramics doped with 0.04 moles of  $\text{GdMnO}_3$  exhibited denser and finer microstructures, which produced a high relative density of  $7.22\text{ g/cm}^3$  (~98% of the theoretic density). Scanning electron microscopy showed uniform distribution of grain and grain boundaries. Comparing with the undoped ceramics, the dielectric properties of the GM-doped PZT specimens are significantly improved. The maximum dielectric constant ( $\epsilon_r=475324$ ) and the minimum dielectric loss (6%) were observed for 0.04 moles of  $\text{GdMnO}_3$ , which indicated that the PZT-GM ceramics are promising to lead to practical applications.

**Keywords:** PZT, dopants, dielectric properties, ceramic, X-ray diffraction, perovskite.

## INTRODUCTION

Perovskite materials have been technologically important because they display interesting dielectric, electromechanical, and ferroelectric properties [1-3]. Piezoelectric ceramics based on lead zirconate titanate (PZT) have been widely used as transducers, sensors, and actuators [4-11]. Lead zirconate titanate  $\text{Pb}(\text{Zr}_x\text{Ti}_{1-x})\text{O}_3$  ceramics are based on a continuous solid solution system of perovskite ferroelectric  $\text{PbTiO}_3$  and antiferroelectric  $\text{PbZrO}_3$  [12, 13]. It is a multi-component solid solution system and a number of compositions are possible by varying Zr:Ti ratio. The structure is rhombohedral for Zr-rich compositions (Zr:Ti >54:46) while it is tetragonal for Ti-rich compositions (Zr:Ti <48:52). Both rhombohedral and tetragonal phases coexist in the intermediate compositions by morphotropic phase boundary (MPB) [14-22]. Adding various dopants within the basic matrix is the method to vary different properties. In general, there are two principal categories of doping: donor or acceptor substitution. Softeners (donors) cause low coercive fields, high remnant polarization, high dielectric constants, maximum coupling factors, high dielectric loss, high mechanical compliance, and reduced aging. Hardeners (acceptors) exhibit high p-type conductivity, reduce dielectric constant, and increase frequency constant, mechanical

quality factors, and aging effects. PZT doped with acceptor ions, such as  $\text{Mn}^{2+}$  (at the B-site), creates oxygen vacancies in the lattice. However, PZT doped with donor ions, such as  $\text{Gd}^{3+}$  (at the A-site), results in vacancies in the A-site known as lead vacancies. Lead vacancies reduce the stress level in the crystalline lattice and allow internal movements in the lattice. Therefore, these effects increase the piezoelectric performance [23]. Portelles et al. [24] have reported very large dielectric permittivity values in the vicinity of the transition temperature. Zhang et al. [22] have observed the best dielectric and piezoelectric properties of  $[(\text{Pb}_{0.95}\text{Sr}_{0.05})_{1-x}\text{Bi}_x][(\text{Zr}_{0.53}\text{Ti}_{0.47})_{1-x}\text{Al}_x]\text{O}_3$  with  $x=0.02$ . PZT powders are usually synthesized by the solid-state reaction process (i.e., calcination method) using mixed oxides as starting materials. Also, the conventional solid-state reacted PZT powders are sintered at very high temperatures [25-27]. The aim of this work is to determine the system with optimized  $\text{GdMnO}_3$  content to achieve higher density and dielectric constant and lower loss tangent ( $\tan\delta$ ) for the construction of high voltage (HV) ceramic capacitors.

## EXPERIMENTAL PROCEDURE

The compositions  $(1-x)\text{Pb}(\text{Zr}_{0.53}\text{Ti}_{0.47})\text{O}_3-x\text{GdMnO}_3$  (PZT-GM) with  $x=0-0.05$  were synthesized using the oxides of elements in the powder form. The raw materials used were  $\text{Pb}_3\text{O}_4$  (Aldrich Chem., 98% purity),  $\text{ZrO}_2$  (Aldrich Chem., 98% purity),  $\text{TiO}_2$  (Travancore Titanium Prod., 98% purity),  $\text{Gd}_2\text{O}_3$  (Biochem, 99.9% purity), and  $\text{Mn}_2\text{O}_3$  (Acros, 99.6%

\*yamna89@yahoo.com

<https://orcid.org/0000-0001-6985-8193>

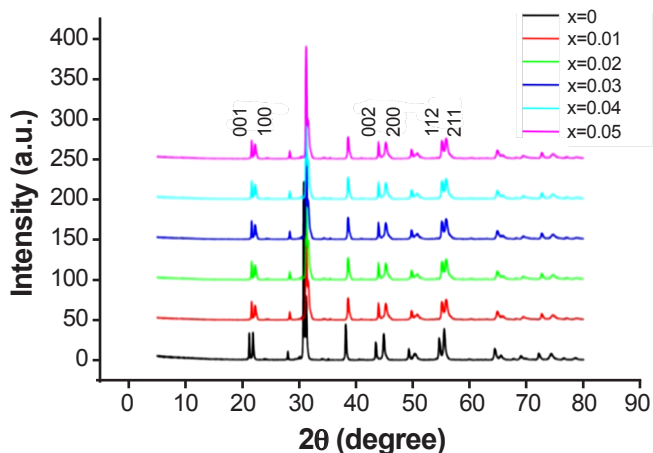


Figure 1: XRD patterns of  $(1-x)\text{Pb}(\text{Zr}_{0.53}\text{Ti}_{0.47})\text{O}_3-x\text{GdMnO}_3$  ceramics with different  $\text{GdMnO}_3$  contents.

urity). The compositions were prepared and processed through a mixed oxide route. The mixtures were weighed stoichiometrically and ball-milled for 6 h. The powders were calcined at 850 °C for 2 h then re-milled for 30 min. After drying, the powders were pressed into disks with a diameter of 10 mm under 1.5 ton using a solution of polyvinyl alcohol (PVA) as a binder. All samples were sintered at 1180 °C for 2 h. The density of the sintered samples was measured by the Archimedes method. The crystal structure of the sintered specimens was analyzed by X-ray diffraction (XRD, D8 Advance, Bruker-AX). The surface morphologies of the ceramics were investigated by scanning electron microscopy (SEM) coupled with energy-dispersive X-ray spectroscopy (EDX, UltraDry, Thermo-Scientific). Dielectric properties were measured from 1 to 100 kHz using an impedance analyzer (SI 1260, Solartron).

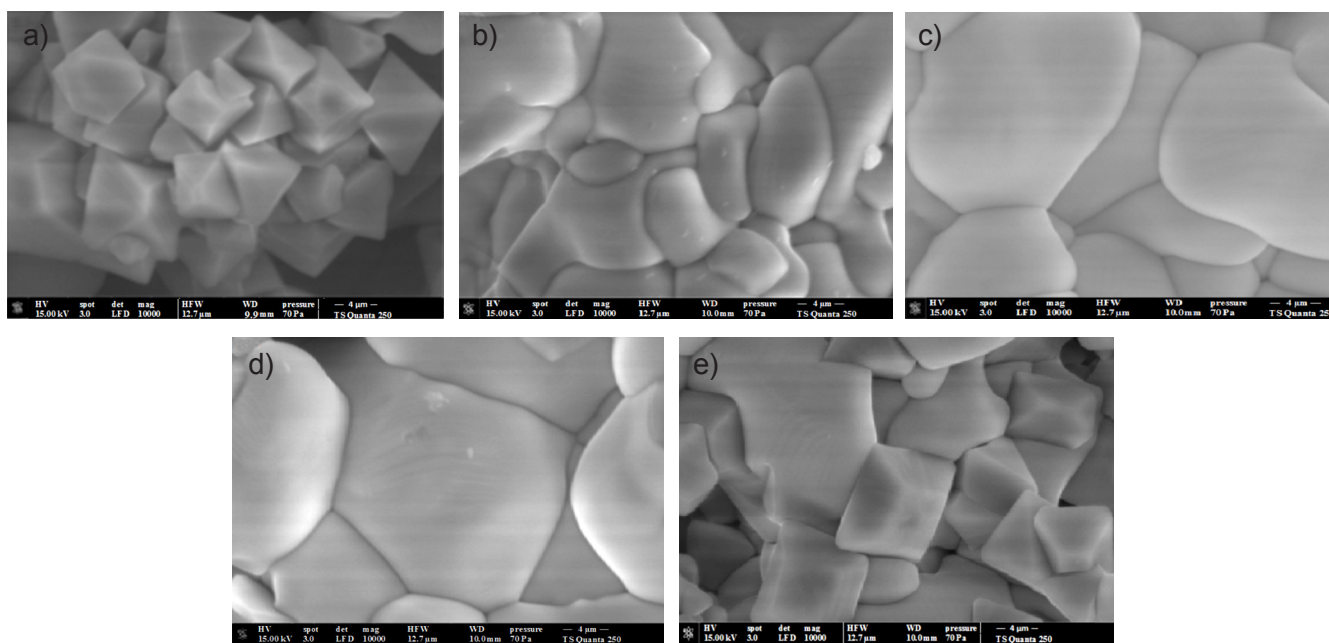


Figure 2: SEM images of  $(1-x)\text{Pb}(\text{Zr}_{0.53}\text{Ti}_{0.47})\text{O}_3-x\text{GdMnO}_3$  ceramics sintered at 1180 °C for: a)  $x=0$ ; b)  $x=0.02$ ; c)  $x=0.03$ ; d)  $x=0.04$ ; and e)  $x=0.05$ .

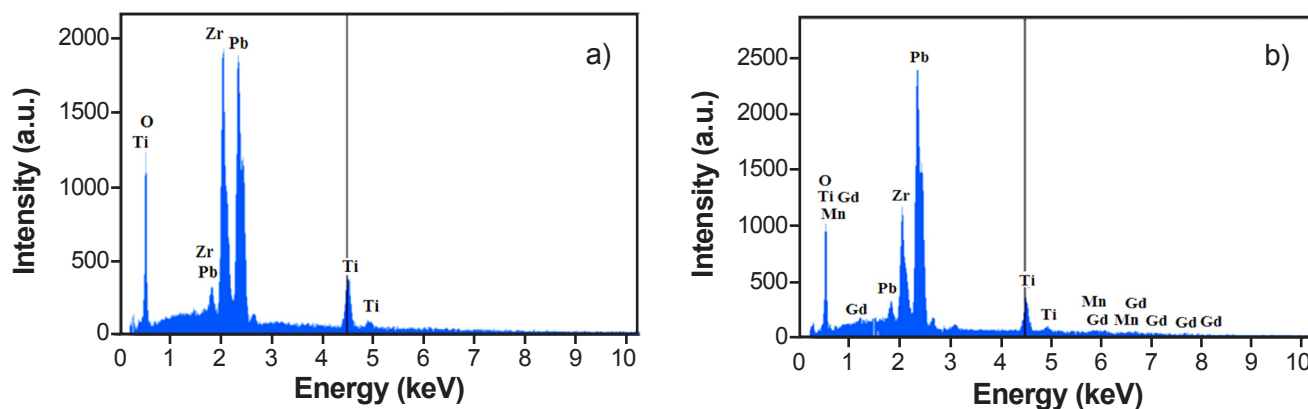


Figure 3: EDX spectra of  $\text{Pb}(\text{Zr}_{0.53}\text{Ti}_{0.47})\text{O}_3$  and  $(1-0.04)\text{Pb}(\text{Zr}_{0.53}\text{Ti}_{0.47})\text{O}_3-0.04\text{GdMnO}_3$ .

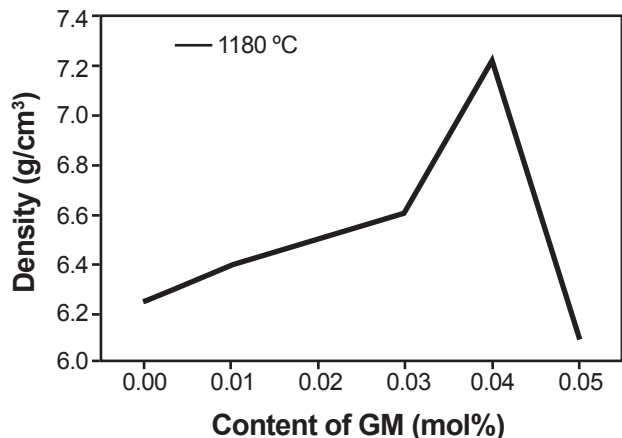


Figure 4: Density of ceramics as a function of GdMnO<sub>3</sub> content.

## RESULTS AND DISCUSSION

**Structural and microstructural properties:** Fig. 1 represents the XRD patterns of  $(1-x)\text{Pb}(\text{Zr}_{0.53}\text{Ti}_{0.47})\text{O}_3-x\text{GdMnO}_3$  ceramics sintered at 1180 °C. The typical tetragonal phase for perovskite at room temperature is typically characterized by separated (100) and (001) peaks at around  $2\theta=22^\circ$  and separated (200) and (002) peaks at around  $2\theta=45^\circ$ , indicating that the formation of the tetragonal phase was not affected by the addition of the GdMnO<sub>3</sub> dopant. The SEM micrographs of GdMnO<sub>3</sub>-doped  $\text{Pb}(\text{Zr}_{0.53}\text{Ti}_{0.47})\text{O}_3$  specimens sintered at 1180 °C are shown in Fig. 2. All the sintered ceramics appeared to be very dense and of a homogeneous granular structure with no grains of the pyrochlore phase, which are identifiable

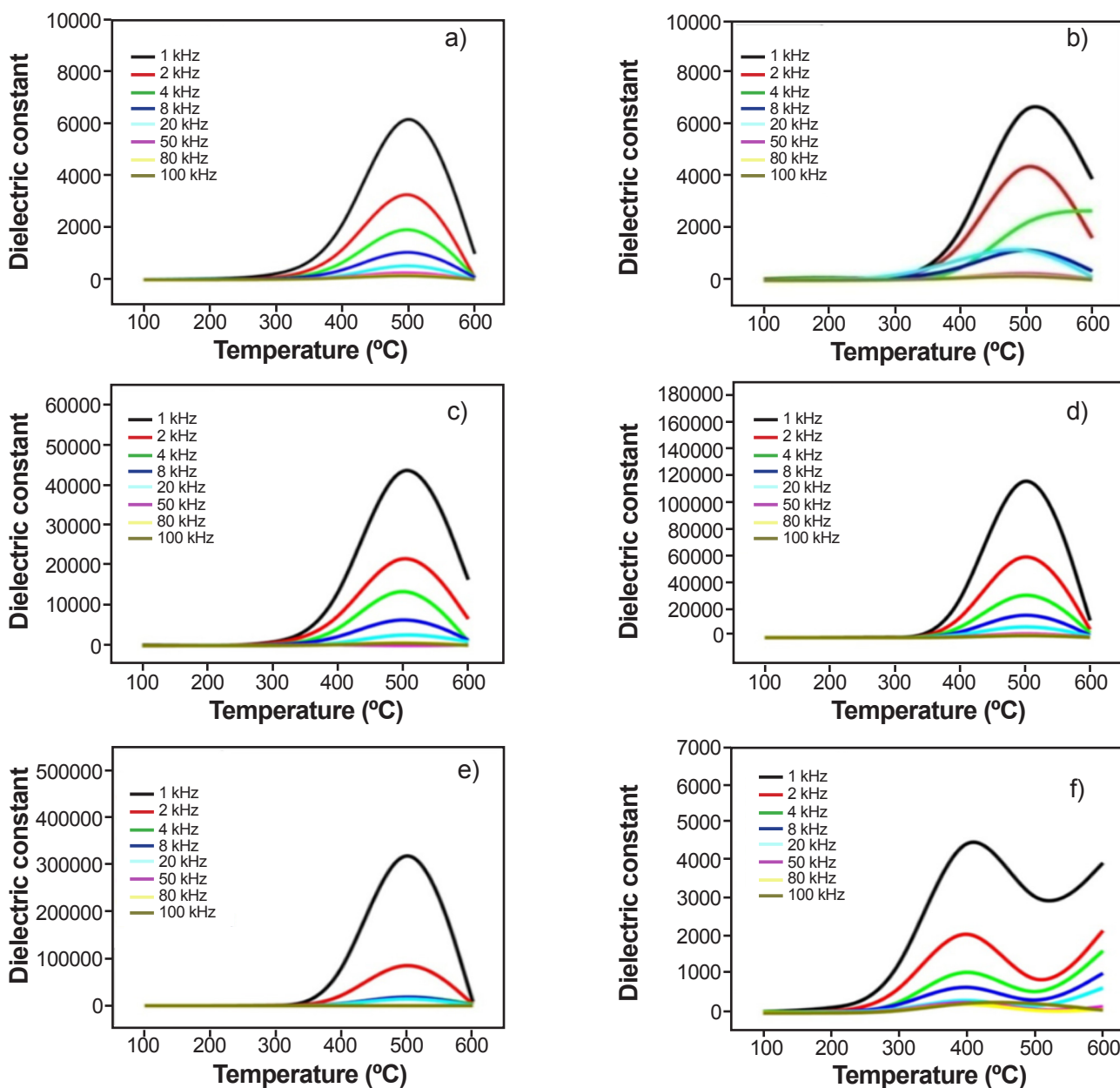


Figure 5: Temperature-frequency dependence of dielectric constant ( $\epsilon_r$ ) of  $(1-x)\text{Pb}(\text{Zr}_{0.53}\text{Ti}_{0.47})\text{O}_3-x\text{GdMnO}_3$  ceramics for: a)  $x=0$ ; b)  $x=0.01$ ; c)  $x=0.02$ ; d)  $x=0.03$ ; e)  $x=0.04$ ; and f)  $x=0.05$ .

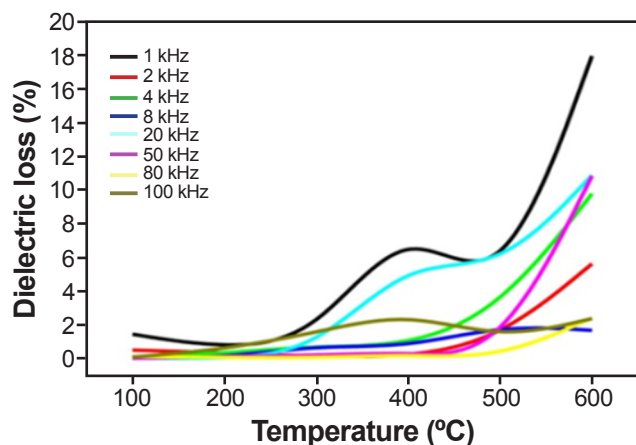


Figure 6: Temperature-frequency dependence of dielectric loss ( $\tan\delta$ ) of  $(1-x)\text{Pb}(\text{Zr}_{0.53}\text{Ti}_{0.47})\text{O}_3-x\text{GdMnO}_3$  ceramics for  $x=0.04$ .

by their pyramidal form [12]. The grain size increased with increasing  $\text{GdMnO}_3$  content, from  $3\ \mu\text{m}$  at  $x=0$  to  $6.10\ \mu\text{m}$  at  $x=0.04$ , and then decrease for  $x>0.04$ . This can be ascribed to suitable amounts of  $\text{GdMnO}_3$  additive that facilitated grain growth and yielded a dense structure for  $0\leq x\leq 0.04$ . The ceramic with 0.04 moles of  $\text{GdMnO}_3$  additive presented a homogeneous microstructure and well-grown grains, which are more applicable for ceramics. The quality of the material increased with increasing density and with increasing sintering temperature [28]. EDX measurements were performed for two different compositions,  $\text{Pb}(\text{Zr}_{0.53}\text{Ti}_{0.47})\text{O}_3$  and  $(1-0.04)\text{Pb}(\text{Zr}_{0.53}\text{Ti}_{0.47})\text{O}_3-0.04\text{GdMnO}_3$ . The EDX spectra (Fig. 3) confirmed the qualitative composition of the obtained samples without the presence of foreign elements [29]. Fig. 4 shows the bulk density of the ceramics as a function of the  $\text{GdMnO}_3$  content sintered at  $1180\ ^\circ\text{C}$ . It can be observed that the density increased with the raise of  $\text{GdMnO}_3$  content and displayed the highest value of  $7.22\ \text{g}/\text{cm}^3$  for the sample with 0.04 moles of  $\text{GdMnO}_3$ . These density variations were in good agreement with the microstructure observed for the various samples.

**Dielectric properties:** Fig. 5 shows the variation of the dielectric constant ( $\epsilon_r$ ) of  $(1-x)\text{Pb}(\text{Zr}_{0.53}\text{Ti}_{0.47})\text{O}_3-x\text{GdMnO}_3$  (having  $\text{GdMnO}_3$  contents of  $x=0, 0.01, 0.02, 0.03, 0.04$ , and  $0.05$ ) with temperature at selected frequencies (1-100 kHz). It can be seen that  $\epsilon_r$  decreased on increasing frequency, which indicated a normal behavior of the ferroelectric and/or dielectric materials. The fall in the dielectric constant arises from the fact that the polarization does not occur instantaneously with the application of the electric field as charges possess inertia. The delay in response towards the impressed alternating electric field leads to loss and hence a decline in dielectric constant. The higher values of  $\epsilon_r$  at lower frequency are due to the simultaneous presence of all types of polarization (space charge, dipolar, ionic, electronic, etc.), which is found to decrease with the increase in frequency. At high frequencies, only electronic polarization exists in the materials [30]. When the temperature of PZT-GM samples was increased,  $\epsilon_r$  first increased slowly and then increased rapidly up to a maximum value ( $\epsilon_{r,\text{max}}$ ). The temperature of

the material corresponding to  $\epsilon_{r,\text{max}}$  is called Curie or critical temperature ( $T_c$ ). As at this  $T_c$ , phase transition takes place between ferroelectric-paraelectric phases so it is also called transition temperature [31, 32]. The relatively high dielectric constant recorded in this study was not frequent in previous work on PZT-modified ceramics. The variation of dielectric loss with temperature and frequencies for compositions with  $x=0.04$  moles at sintering temperature of  $1180\ ^\circ\text{C}$  are shown in Fig. 6. When the temperature rises, the orientation of dipoles is facilitated and this increased the loss tangent ( $\tan\delta$ ). At high temperatures, the dielectric losses caused by the dipole mechanism reached their maximum value and the degree of dipole orientation increased. Also, we observed that the dielectric loss decreased with augmentation in frequency [33].

## CONCLUSIONS

Ceramic samples of  $(1-x)\text{Pb}(\text{Zr}_{0.53}\text{Ti}_{0.47})\text{O}_3-x\text{GdMnO}_3$  solid solution system were prepared by a solid-state reaction method. The structure, microstructure, and dielectric properties were investigated systematically. The results indicated that GM-modified ceramics exhibited the tetragonal phase. A dense and uniform microstructure was obtained for the PZT doped with 0.04 moles of  $\text{GdMnO}_3$ . The maximum dielectric constant ( $\epsilon_r=475324$ ) and the minimum dielectric loss (6%) were observed for 0.04 moles of  $\text{GdMnO}_3$ . From the results obtained, the properties of the compositionally modified PZT ceramics can also be tailored over a wide range by changing the dopant compositions to meet the specific requirements for different applications.

## REFERENCES

- [1] A.J. Joseph, S. Goel, A. Hussain, B. Kumar, *Ceram. Int.* **43** (2017) 16676.
- [2] G.H. Haertling, *J. Am. Ceram. Soc.* **82** (1999) 797.
- [3] M. Gabilondo, I.N. Burgos, M. Azcona, F. Castro, *Ceram. Int.* **45** (2019) 23149.
- [4] R. Samad, M.D. Rather, K. Asokan, B. Want, *J. Mater. Sci. Mater. Electr.* **29** (2018) 4226.
- [5] J. Peng, J. Zeng, G. Li, L. Zheng, X. Ruan, X. Huang, D. Zhang, *Ceram. Int.* **43** (2017) 13233.
- [6] X. Luo, J. Zeng, X. Shi, L. Zheng, K. Zhao, Z. Man, G. Li, *Ceram. Int.* **44** (2018) 8456.
- [7] H. Liu, R. Nie, Y. Yue, Q. Chen, *Ceram. Int.* **41** (2015) 11359.
- [8] B. Cherdhirunkorn, S. Surakulananta, J. Tangsritrakul, D. Hall, S. Intarasiri, *Results Phys.* **16** (2020) 102851.
- [9] J. Gao, X. Hu, Y. Liu, Y. Wang, X. Ke, D. Wang, L. Zhong, X. Ren, *J. Phys. Chem. C* **121** (2017) 14322.
- [10] N. Buatip, M. Dhanunjaya, P. Amonpattaratkit, P. Pomyai, T. Sonklin, K. Reichmann, P. Janphaung, S. Pojprapai, *Radiat. Phys. Chem.* **172** (2020) 108770.
- [11] J. Hao, W. Li, J. Zhai, H. Chen, *Mater. Sci. Eng. R* **135** (2019) 1.
- [12] L. Ben Amor, A. Boutarfaia, O. Bentouila, *J. Appl. Eng.*

- Sci. Technol. **4** (2018) 21.
- [13] N. Zelikha, B. Ahmed, K. Amel, M. Hayet, B. Karima, A. Malika, A. Nora, M. Abdelhek, Int. J. Pharm. Chem. Biol. Sci. **4** (2014) 438.
- [14] P.K. Panda, B. Sahoo, Ferroelectrics **474** (2015) 128.
- [15] T. Li, C. Liu, X. Ke, X. Liu, L. He, P. Shi, X. Ben, Acta Mater. **182** (2020) 39.
- [16] C.A. Randall, N. Kim, J.P. Kucera, W. Cao, T.R. Shrout, J. Am. Ceram. Soc. **81** (1998) 677.
- [17] J. Walker, H. Simons, D.O. Alikin, A.P. Turygin, V.Y. Shur, Sci. Rep. **6** (2016) 19630.
- [18] J.D. Bobić, M. Ivanov, N.I. Ilić, A.S. Dzunuzović, M.M.V. Petrović, J. Banys, Ceram. Int. **44** (2018) 6551.
- [19] E. Lupi, A. Ghosh, S. Saremi, S.-L. Hsu, S. Pandya, Adv. Electr. Mater. **6** (2020) 1901395.
- [20] G.G. Peng, D.Y. Zheng, S.M. Hu, H. Zhao, C. Cheng, J. Zhang, J. Mater. Sci. Mater. Electr. **27** (2016) 5509.
- [21] A.S. Karapuzha, N.K. James, H. Khanbareh, S. van der Zwaag, W.A. Groen, Ferroelectrics **504** (2016) 160.
- [22] D. Zhang, J. Zeng, L. Zheng, X. Ruan, X. Shi, Ferroelectrics **534** (2018) 212.
- [23] F. Kahoul, L. Hamzioui, Z. Necira, A. Boutarfaia, Energy Procedia **36** (2013) 1050.
- [24] J. Portelles, N.S. Almodovar, J. Fuentes, O. Raymond, J. Heiras, J. Appl. Phys. **104** (2008) 73511.
- [25] D. Bochenek, P. Niemiec, I. Szafraniak-Wiza, Materials **12** (2019) 3301.
- [26] S. Adel, B. Cherifa, D. Elhak, B. Mounira, Bol. Soc. Esp. Ceram. V. **57** (2017) 124.
- [27] M.S. Silva, R.G. Dias, E.F. Souza, M. Cilense, Mater. Sci. Forum **869** (2016) 8.
- [28] A. Boutarfaia, Ceram. Int. **26** (2000) 583.
- [29] M. Khacheba, N. Abdessalem, A. Hamdi, H.K. Hemakhem, J. Mater. Sci. Mater. Electr. **31** (2020) 361.
- [30] C.J.F. Bottcher, *Theory of electric polarization*, Elsevier (1952).
- [31] Z. He, J. Ma, R. Zhang, T. Li, J. Eur. Ceram. Soc. **23** (2002) 1943.
- [32] Y. Xu, *Ferroelectric materials and their applications*, North Holland, Amsterdam (1991).
- [33] N.K. Singh, Pritam Kumar, A. Kumar, S. Sharma, J. Eng. Technol. Res. **4** (2012) 104.  
(Rec. 15/04/2021, Rev. 29/05/2021, 13/07/2021, Ac. 17/07/2021)

